arXiv:0905.1385v1 [cs.CR] 9 May 2009

Making Hand Geometry Verification System More Accurate Using Time Series Representation with R-K Band Learning

Vit Niennattrakul Chotirat Ann Ratanamahatana

Department of Computer Engineering, Chulalongkorn University
Phayathai Rd., Pathumwan, Bangkok 10330 Thailand
E-mail: {g49vnn, ann}@cp.eng.chula.ac.th

Abstract

At present, applications of biometrics are rapidly increasing due to inconveniences in using traditional passwords and physical keys. Hand geometry, one of the most well-known biometrics, is implemented in many verification systems with various feature extraction methods. In recent work, a hand geometry verification system using time series conversion techniques and Dynamic Time Warping (DTW) distance measure with Sakoe-Chiba band has been proposed. This system demonstrates many advantages, especially ease of implementation and small storage space requirement using time series representation. In this paper, we propose a novel hand geometry verification system that exploits DTW distance measure and R-K band learning to further improve the system performance. Finally, our evaluation reveals that our proposed system outperforms the current system by a wide margin, in terms of False Acceptance Rate (FAR), False Rejection Rate (FRR), and Total Success Rate (TSR) at Equal Error Rate (EER).

1. Introduction

Nowadays, biometrics is gradually used in place of traditional passwords and physical keys simply because the passwords could be forgotten and the physical keys could be lost or stolen. On the other hand, many parts of human organs or characteristics such as a fingerprint, hand geometry, an iris, voice, a face profile, and a signature, are unique enough to be used for person identification purposes. Specifically, Table 1 shows a comparison among various biometrics based on seven attributes [11, 13], i.e., universality, uniqueness, permanence, collectability, performance, acceptability, and circumvention.

A biometric authentication system can be categorized into two main functionalities [13] – identification and verification. For identification, a system receives an image from an input sensor, extracts features, and queries from a database for the best match. If the input image is too different from the best retrieved template, the system rejects. Otherwise, it accepts and identifies the input's identity. Unlike identification, a verification system requires a user identity as an additional input. Instead of querying from all the templates in the database, the verification system queries on only the claimed user's own templates. Matching only on much smaller set of templates generally makes the verification system much more accurate than the identification system.

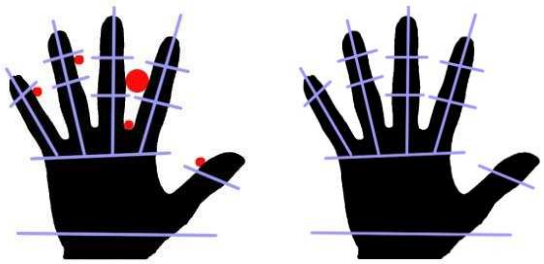

(a) (b)

Figure 1. Images acquired from (a) a peg-fixed system and (b) a peg-free system.

At present, many hand geometry authentication systems are implemented both in identification and verification tasks due to the ease of sample collection, relatively low hardware costs, and availability of various feature extraction algorithms. Specifically, two system environments are designed, shown in Figure 1, i.e., a peg-fixed system [24, 15, 26, 29] and a peg-free system [5, 9, 6, 8, 20, 16, 1, 27, 28, 19, 3]. The peg-fixed system uses pins attached on a plate to align hand's position properly. On the other hand, in the peg-free system, no pin is needed. To transform an input image to computable numerical features, many extraction methodologies have been proposed [16, 28, 4, 12, 25, 18, 10]. Unfortunately, these extracted features techniques are quite

Table 1. Various biometric comparison based on seven attributes [13]

Biometrics	Universality	Uniqueness	Permanence	Collectability	Performance	Acceptability	Circumvention
Face	High	Low	Medium	High	Low	High	Low
Fingerprint	Medium	High	High	Medium	High	Medium	High
Hand geometry	Medium	Medium	Medium	High	Medium	Medium	Medium
Keystroke	Low	Low	Low	Medium	Low	Medium	Medium
Iris	High	High	High	Medium	High	Low	High
Signature	Low	Low	Low	High	Low	Medium	Low
Voice	Medium	Low	Low	Medium	Low	Medium	Low

computationally expensive and the system may fail to extract features in some of the hand configurations.

Recently, a hand geometry verification system using a time series representation [17] has been proposed. Some of its advantages include small storage space requirement and ease of implementation. To compare similarity between two time series data, Dynamic Time Warping distance measure with Sakoe-Chiba band [23] is used.

In this paper, we extend this previous work further. Instead of using Sakoe-Chiba band, R-K bands [21] are used and are assigned to each user's templates with calculated threshold values. This novel hand geometry verification system significantly increases overall system performances, especially, reduction in False Acceptance Rate (FAR) and False Rejection Rate (FRR) at Equal Error Rate (EER).

The rest of the paper is organized as follows. Our proposed hand geometry verification system is described in Section 2. Section 3 discusses our evaluation method and shows the experimental results. Finally, in Section 4, we conclude our work and provide some suggestions.

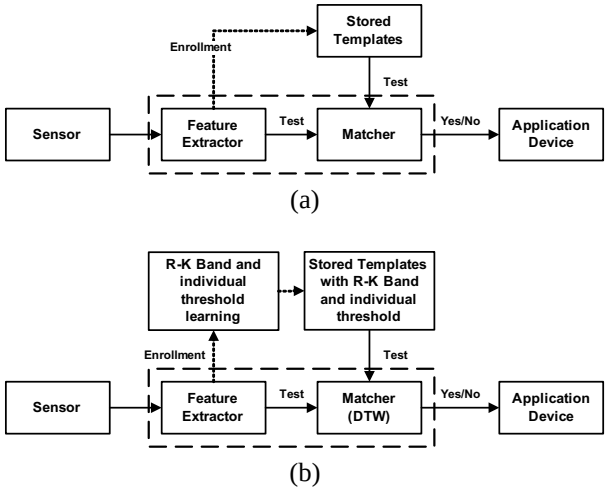

Figure 2. Overviews of (a) a typical biometric verification system and (b) our proposed hand geometry verification system.

2. Hand Geometry Verification System

Typical verification system usually consists of five major components [13], i.e., a sensor, a feature extractor, a matcher, a stored template, and an application device with two functions – enrollment and testing, as shown in Figure 2 (a). First, data are acquired from a sensor, and then the input data are sent to a feature extractor to transform the data to numerical features. If the system is in an enrollment step, input features (from the feature extractor) will be added to a database as a stored template labeled with a user's identity. During the test phase, a matcher retrieves the stored templates corresponding only to the claimed username, and a distance measure is used to calculate similarity between the input features and these retrieved templates. If the distance is less than a pre-defined threshold, the system accepts; otherwise, it rejects.

Our proposed system, extended from the typical verification system, consists of six components – a hand scanner, a feature extractor, R-K band and user's individual threshold learning, stored templates with R-K band and user's individual threshold, a matcher, and an application device. A scanner first acquires an input hand image, and then time series data is extracted from the input image using the feature extractor; a centroid-based [14] or an angle-based [7] technique is used for the time series conversion. After extraction has finished and the system has been in the enrollment step, an R-K band and user's individual threshold is learned and stored. In the testing step, user's templates with the learned R-K band and user's threshold are retrieved. The matcher uses DTW distance measure with this learned R-K band to find the best match within this stored set of templates. Finally, the measured distance is compared to that particular user's threshold multiplied by a system-wide threshold to grant or deny access to an application device. An overview of our proposed system is shown in Figure 2 (b).

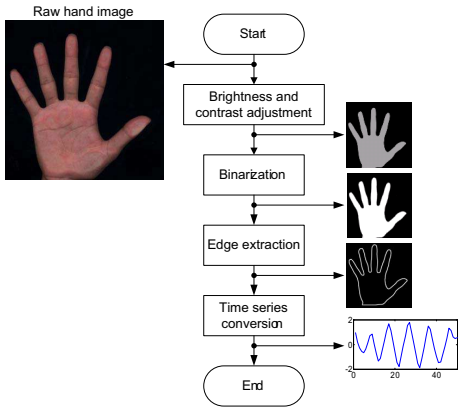

Figure 3. Steps of converting a raw hand image to time series data.

2.1. Feature Extractor

The feature extractor [17] (shown in Figure 3) converts acquired images to time series according to the following steps, i.e., brightness and contrast adjustment, binarization, edge extraction, and time series conversion.

Brightness and Contrast Adjustment. After an original color raw image is obtained, it will be transformed into a grayscaled image. Then, the system will adjust its brightness and contrast to the quality that is suitable for the binarization step.

Binarization. After brightness and contrast adjustment, some image pixels may not be pure black or white. So, we binarize each pixel into solid black or white, represented by '0' and '1', respectively. The binarization function is defined as follows

$$B(x,y) = \begin{cases} 1 & \text{if } I_{xy} \geq t \\ 0 & \text{otherwise} \end{cases} \quad (1)$$

where I_{xy} is the intensity ranging from 0 to 1 at pixel (x, y), and t is the specified threshold for binarization. The default threshold value for the grayscale image is simply set to 0.5.

Edge Extraction. The goal in this step is to find an edge sequence from a binarized hand image by using boundary extraction algorithm [7]. The algorithm precisely starts scanning of each pixel from the top left of the image to the bottom right of the image. Once it finds the first black pixel, it stops scanning, and then traces along the edge in a clockwise direction until it returns to the starting pixel.

Time Series Conversion. In this step, we calculate the edge sequence, and transform hand's shape into time series data by using two techniques, i.e., an angle-based technique [7] and a centroid-based technique [14]. In the angle-based technique, for each pixel index i, we create two tangent lines – forward and backward tangents. The forward line is created by drawing a straight line from the pixel index i to the pixel index $i + \delta$, and the backward line is created by drawing a straight line from the pixel index i to the pixel index $i - \delta$. Note that the δ value depends on the size of the image; the larger the δ value, the smoother the time series, and vice versa. In our experiment, the default value of δ is set to 10. After that we record the angle formed by these two lines as time series' amplitude, as shown in Figure 4 (a). In the centroid-based technique, we first locate the hand's centroid. Once the centroid is obtained, we simply plot the Euclidean distance from each pixel position to the centroid position. The general idea of centroid-based conversion is shown in Figure 4 (b).

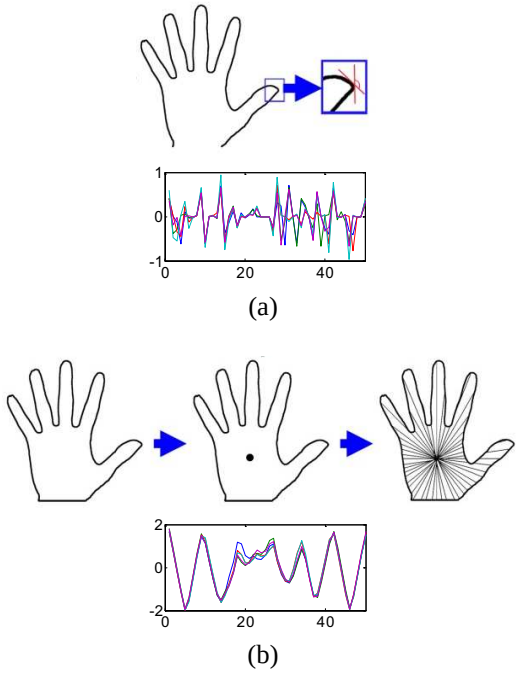

Figure 4. General ideas of (a) an angle-based conversion technique and (b) a centroid-based conversion technique.

2.2. Dynamic Time Warping (DTW) Distance Measure

Dynamic Time Warping (DTW) [2, 22] distance measure is a well-known similarity measure based on shape. It uses a dynamic programming technique to find all possible warping paths, and selects the one with the minimum distance between two time series. To calculate the distance, it first creates a distance matrix, where each element in the matrix is a cumulative distance of the minimum of three surrounding neighbors. Suppose we have two time series, a sequence $Q = \langle q_1, q_2, \ldots, q_i, \ldots, q_n \rangle$ and a sequence

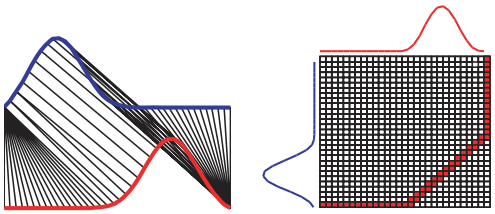

Figure 5. DTW without using global constraint may introduce an unwanted warping.

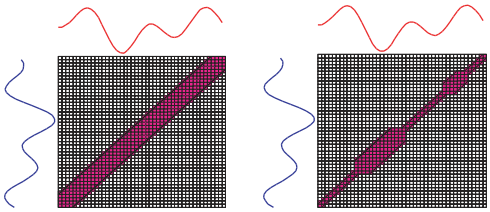

(a) (b)

Figure 6. Global constraint examples of (a) Sakoe-Chiba band and (b) Ratanamahatana-Keogh band.

$C = \langle c_1, c_2, \ldots, c_j, \ldots, c_m \rangle$. First, we create an n-by-m matrix where every (i, j) element of the matrix is the cumulative distance of the distance at (i, j) and the minimum of three neighboring elements, where $1 \leq i \leq n$ and $1 \leq j \leq m$. We can define the (i, j) element, γ_{ij}, of the matrix as:

$$\gamma_{i,j} = d_{ij} + \min\{\gamma_{i-1,j-1}, \gamma_{i-1,j}, \gamma_{i,j-1}\} \quad (2)$$

where $d_{ij} = (c_i - q_j)^2$ is the squared distance of q_i and c_j, and $\gamma_{i,j}$ is the summation of d_{ij} and the minimum cumulative distance of three elements surrounding the (i, j) element. Then, to find an optimal path, we choose the path that yields a minimum cumulative distance at (n, m), which is defined as:

$$DTW(Q, C) = \min_{\forall W \in \mathbb{W}} \left\{ \sqrt[p]{\sum_{k=1}^{K} d_{w_k}} \right. \quad (3)$$

where $\mathbb{W}$ is a set of all possible warping paths, w_k is (i, j) at k^{th} element of a warping path, and K is the length of the warping path.

In reality, DTW may not give the best mapping according to our need because it will try its best to find the minimum distance though it may generate an unwanted path. For example, in Figure 5, without a global constraint, DTW will find its optimal mapping between two time series. However, in many cases, this is probably not what we intend, where the two time series are expected to be of different classes. We can resolve this problem by limiting permissible warping paths using a global constraint. A well-known global constraints, Sakoe-Chiba band (S-C band) [23] and a recent representation, Ratanamahatana-Keogh band (R-K band) [21], have been proposed. Figure 6 shows an example for each type of the constraints.

2.3. R-K Band Learning

Ratanamahatana-Keogh band (R-K band) [21] is a general model of a global constraint specified by a one-dimensional array R, i.e., $R = \langle r_1, r_2, \ldots, r_i, \ldots, r_n \rangle$ where n is the length of time series, and r_i is the height above the diagonal in y direction and the width to the right of the diagonal in x direction. Each r_i value is arbitrary, therefore R-K band is also an arbitrary-shape global constraint, as shown in Figure 6 (b). Note that when $r_i = 0$, where $1 \leq i \leq n$, this R-K band represents the Euclidean distance, and when $r_i = n$, $1 \leq i \leq n$, this R-K band represents the classic DTW distance with no global constraint. The R-K band is also able to represent the S-C band by giving all $r_i = c$, where c is the width of a global constraint. Moreover, the R-K band is a multi band model which can effectively be used to represent one band for each class of the data. This flexibility is a great advantage; however, the higher the number of classes, the larger the time complexity, as we have to search through such a large space.

Since determining the optimal R-K band for each training set is quite computationally intensive, a hill climbing and heuristic functions have been introduced to guide which part of space should be evaluated. A space is defined as a segment of a band to be increased or decreased. In the original work, two heuristic functions, accuracy metric and distance metric, are used to evaluate a state. The accuracy metric is evaluated from the training accuracy using leave-one-out 1-NN, and the distance metric is a ratio of the mean DTW distances of correctly classified and incorrectly classified objects.

Two searching directions are considered, i.e., a forward search, and a backward search. In a forward search, we start from the Euclidean distance (all r_i values in R equal to 0), and parts of the band are gradually increased in each searching step. In the case where two bands have the same heuristic value, a wider band is selected. On the other hand, in a backward search, we start from a very large band (all r_i values in R equal to n, where n is the length of the time series), and parts of the band are gradually decreased in each searching step. If two bands have the same heuristic value, the tighter band is chosen.

Our learning algorithm first starts from enqueuing the starting- and ending-parts of the R-K Band. In each itera-

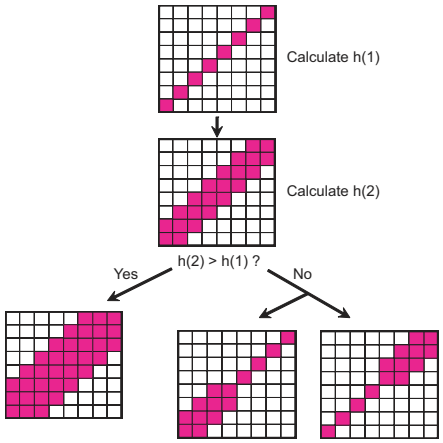

Figure 7. An illustration of the concept in R-K band forward searching algorithm. [21]

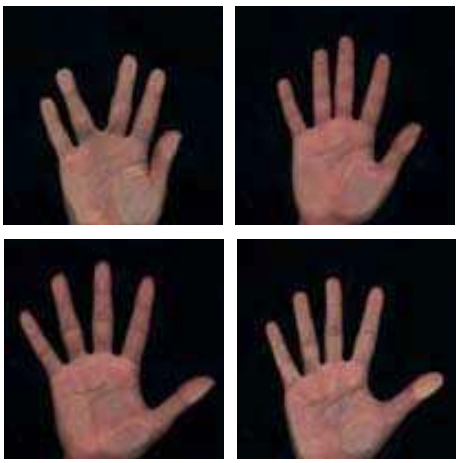

Figure 8. Examples of input hand images from four different people.

Table 2. The pseudo code for multiple R-K bands learning.

FUNCTION [$band$] = LEARNING[T,$threshold$]

```
1   N= size of T;
2   L= length of data in T;
3   initialize band_i for i = 1 to c;
4   foreachclass i = 1 to c
5     enqueue(1, L, Queue_i);
6   endfor
7   best_evaluate = evaluate(T, band);
8   while !empty(Queue)
9     foreachclass i = 1 to c
10      if !empty(Queue_i)
11        [start, end] = dequeue(Queue_i)
12        adjustable = adjust(bandi, start, end);
13        if adjustable
14          evaluate= evaluate(T, band);
15          if evaluate > best_evaluate
16            best_evaluate = evaluate;
17            enqueue(start, end, Queue_i);
18          else
19            undo_adjustment(band_i, start, end);
20            if (start – end) / 2 ≥ threshold
21              enqueue(start, mid-1, Queue_i);
22              enqueue(mid, end, Queue_i);
23            endif
24          endif
25        endif
26      endif
27    endfor
28  endwhile
```

tion, these values are dequeued and used as a boundary for a band expansion/reduction. The adjusted band is then evaluated. If a heuristic value is higher than the current best heuristic value, the same start and end values are enqueued. If not, this part is further divided into two equal subparts before being enqueued, as shown in Figure 7. The iterations are continued until a termination condition is met. Table 2 shows the pseudo code for this multiple R-K bands learning.

3. Experimental Evaluation

The dataset is collected from 21 different persons, 6-7 images per person, in a total of 128 images, using a color scanner with 1200x1200 pixel resolution. Examples of input hand images are shown in Figure 8.

After that all images are converted into time series data by applying two time series conversion techniques – a centroid-based conversion technique and an angle-based conversion technique, and then time series data are down-sampled to 50 data points. Examples of converted time series data using the centroid-based technique and the angle-based technique are shown in Figure 9 (a) and (b), respectively.

To evaluate the system's performance, we use three well-known measurements, i.e., False Rejection Rate (FRR), False Acceptance Rate (FAR), and Total Success Rate (TSR). They can be calculated by the following equations.

$$FRR = \frac{\#RejectGenuineClaims}{Total\#GenuineAccess} \cdot 100\% \qquad (4)$$

$$FAR = \frac{\#AcceptImposterClaims}{Total\#ImposterAccess} \cdot 100\% \qquad (5)$$

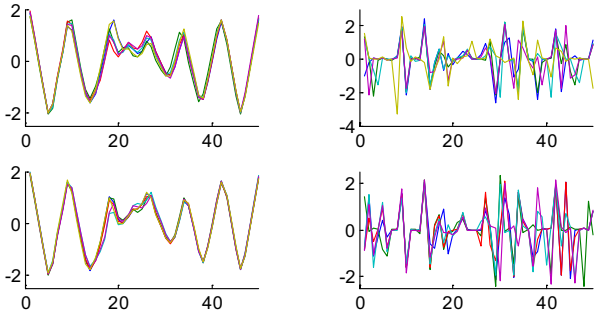

(a) (b)

Figure 9. Time series data examples after the conversion using (a) the centroid-based technique and (b) the angle-based technique.

	Previous approach	
	Centroid-based technique	**Angle-based technique**
FAR	14.06%	25.59%
FRR	14.30%	25.78%
TSR	85.71%	72.99%

	Proposed method	
	Centroid-based techniques	**Angle-based techniques**
FAR	11.72%	23.67%
FRR	11.91%	23.43%
TSR	88.10%	76.33%

Table 3. The comparison of FAR, FRR, and TSR among different approaches at EER.

$$TSR = \left(1 - \frac{FAR + FRR}{Total\#Access}\right) \cdot 100\% \qquad (6)$$

To get the best performance, two parameters are varied – a systemwide (global) threshold and a conversion technique. An experimental result at the Equal Error Rate (EER) point, where FAR equals to FRR, is shown in Table 3. Note that the lower the EER value, the higher the accuracy of the biometric system. To further illustrate our overall performance, we also show their ROC (Receive Operating Characteristic) curves (shown in Figure 10). At the EER, our proposed method gets better performance (lower FAR, lower FRR, and higher TSR) in all evaluation metrics.

4. Conclusion

We have demonstrated our novel hand geometry verification system by using time series data as an image representation and comparing time series using Dynamic Time

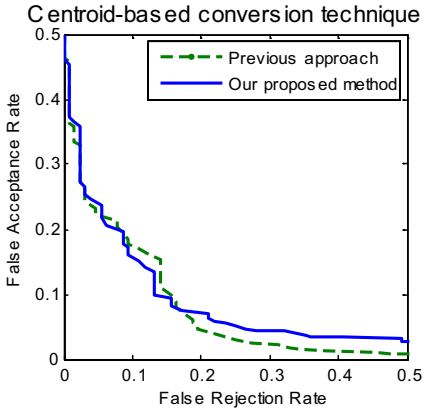

(a)

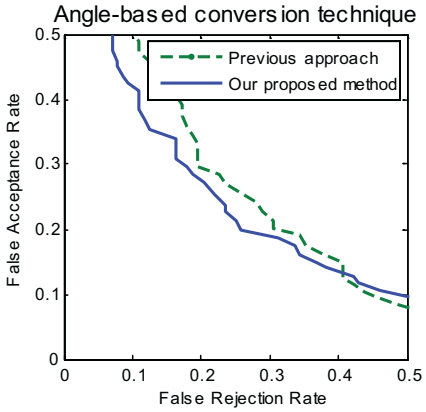

(b)

Figure 10. The ROC curves of our proposed system comparing with the previous one using (a) the centroid-based conversion technique and (b) the angle-based conversion technique.

Warping distance measure with the R-K band. In the proposed system, two time series conversion techniques are applied, i.e., the centroid-based conversion technique and the angle-based technique. Our experiment reveals that the centroid-based technique generally outperforms the angle-based technique by achieving lower EER and higher TSR. Finally, by comparing the result with the previous approach, our proposed system gets much higher performance.

For future work, this hand geometry verification system can be extended to be a multi-biometric system. The fingerprint and palm print can be verified together in order to boost up the system's performance.

References

[1] M. Arif, T. Brouard, and N. Vincent. Personal identification and verification by hand recognition. In *Proceedings of the 2006 IEEE International Conference on Engineering of Intelligent Systems (INES 2006)*, pages 1–6, London, UK, June 26-28 2006.

[2] D. J. Berndt and J. Clifford. Using dynamic time warping to find patterns in time series. In *the 1994 AAAI Workshop on Knowledge Discovery in Databases*, pages 359–370, Seattle, Washington, July 1994.

[3] G. Boreki and A. Zimmer. Hand geometry: A new approach for feature extraction. In *Proceedings of 4th IEEE Workshop on Automatic Identification Advanced Technologies (AutoID 2005)*, pages 149–154, 2005.

[4] Y. Bulatov, S. Jambawalikar, P. Kumar, and S. Sethia. Hand recognition using geometric classifiers. In *Proceedings of the First International Conference on Biometric Authentication (ICBA 2004)*, pages 753–759, Hong Kong, China, July 15-17 2004.

[5] J. Doublet, O. Lepetit, and M. Revenu. Contact less hand recognition using shape and texture features. In *Proceedings of 8th International Conference on Signal Processing (CISP 2006)*, volume 3, Toulouse, France, December 16-20 2006.

[6] M. Faúndez-Zanuy and G. M. N. Mérida. Biometric identification by means of hand geometry and a neural net classifier. In *Proceedings of 8th International Work-Conference on Artificial Neural Networks (IWANN 2005)*, pages 1172–1179, Vilanova i la Geltrú, Barcelona, Spain, June 8-10 2005.

[7] A. Gandhi. Content-based image retrieval: Plant species identification. Master's thesis, Oregon State University, 2002.

[8] S. Gonzalez, C. Travieso, J. Alonso, and M. Ferrer. Automatic biometric identification system by hand geometry. In *Proceedings of IEEE 37th Annual 2003 International Carnahan Conference on Security Technology (ICCST 2003)*, pages 281–284, Taipei, Taiwan, ROC, October 14-16 2003.

[9] J. Hashemi and E. Fatemizadeh. Biometric identification through hand geometry. In *Proceedings of the International Conference on Computer as a Tool (EUROCON 2005)*, volume 2, pages 1011–1014, November 21-24, Belgrade, Sebia and Montenegro 2005.

[10] A. Jain, A. Ross, and S. Pankanti. A prototype hand geometry-based verification system. In *Proceedings of 2nd International Conference on Audio- and Video-based Biometric Person Authentication (AVBPA '99)*, pages 166–171, Washington D.C., USA, March 22-23 1999.

[11] A. K. Jain. Biometric recognition: How do i know who you are? In *Proceedings of 13th International Conference on Image Analysis and Processing (ICIAP 2005)*, pages 19–26, Cagliari, Italy, September 6-8 2005.

[12] A. K. Jain and N. Duta. Deformable matching of hand shapes for user verification. In *Proceedings of the 1999 International Conference on Image Processing (ICIP '99)*, pages 857–861, Kobe, Japan, October 24-28 1999.

[13] A. K. Jain, A. Ross, and S. Pankanti. Biometrics: a tool for information security. *IEEE Transactions on Information Forensics and Security*, 1(2):125–143, 2006.

[14] E. J. Keogh, L. Wei, X. Xi, S.-H. Lee, and M. Vlachos. LB_Keogh supports exact indexing of shapes under rotation invariance with arbitrary representations and distance measures. In *Proceedings of the 32nd International Conference on Very Large Data Bases (VLDB 2006)*, pages 882–893, Seoul, Korea, September 12-15 2006.

[15] E. Kukula and S. Elliott. Implementation of hand geometry at purdue university's recreational center: an analysis of user perspectives and system performance. In *Proceedings of 39th Annual 2005 International Carnahan Conference on Security Technology (CCST 2005)*, pages 83–88, Oct. 2005.

[16] A. Kumar, D. C. M. Wong, H. C. Shen, and A. K. Jain. Personal verification using palmprint and hand geometry biometric. In *Proceedings of 4th International Conference on Audio-and Video-Based Biometrie Person Authentication (AVBPA 2003)*, pages 668–678, 2003.

[17] V. Niennattrakul, D. Wanichsan, and C. A. Ratanamahatana. Hand geometry verification using time series representation. In *Proceedings of 11th International Conference on Knowledge-Based Intelligent Information and Engineering Systems (KES 2007)*, pages 824–831, 2007.

[18] C. Öden, A. Erçil, and B. Büke. Combining implicit polynomials and geometric features for hand recognition. *Pattern Recognition Letters*, 24(13):2145–2152, 2003.

[19] C. Öden, A. Erçil, V. T. Yildiz, H. Kirmizitas, and B. Büke. Hand recognition using implicit polynomials and geometric features. In *Proceedings of the Third International Conference on Audio- and Video-Based Biometric Person Authentication (AVBPA 2001)*, pages 336–341, Halmstad, Sweden, June 6-8 2001.

[20] M. G. K. Ong, T. Connie, A. T. B. Jin, and D. N. C. Ling. A single-sensor hand geometry and palmprint verification system. In *Proceedings of the 2003 ACM SIGMM workshop on Biometrics methods and applications (WBMA 2003)*, pages 100–106, New York, NY, USA, 2003. ACM.

[21] C. A. Ratanamahatana and E. J. Keogh. Making time-series classification more accurate using learned constraints. In *Proceedings of the Fourth SIAM International Conference on Data Mining (SDM 2004)*, pages 11–22, Lake Buena Vista, Florida, USA, April 22-24 2004.

[22] C. A. Ratanamahatana and E. J. Keogh. Three myths about dynamic time warping data mining. In *Proceedings of 2005 SIAM International Data Mining Conference (SDM 2005)*, pages 506–510, Newport Beach, CL, USA, April 21-23 2005.

[23] H. Sakoe and S. Chiba. Dynamic programming algorithm optimization for spoken word recognition. *IEEE Transactions on Acoustics, Speech, and Signal Processing*, 26(1):43–49, 1978.

[24] R. Sanchez-Reillo and A. Gonzalez-Marcos. Access control system with hand geometry verification and smart cards. *IEEE Aerospace and Electronic Systems Magazine*, 15(2):45–48, Feb 2000.

[25] R. Sánchez-Reillo, C. Sanchez-Avila, and A. González-Marcos. Biometric identification through hand geometry measurements. *IEEE Transactions on Pattern Analysis and Machine Intelligence (TPAMI)*, 22(10):1168–1171, 2000.

[26] L. Stasiak. Support vector machine for hand geometry-based identity verification system. *Photonics Applications*

in Astronomy, Communications, Industry, and High-Energy Physics Experiments 2006, 6347(1):634725, 2006.

[27] F. Yang, B. Ma, Q. xia Wang, and D. Yao. Information fusion of biometrics based-on fingerprint, hand-geometry and palm-print. In *Proceedings of 2007 IEEE Workshop on Automatic Identification Advanced Technologies (AutoID 2007)*, pages 247–252, Alghero, Italy, June 7-8 2007.

[28] E. Yörük, E. Konukoglu, B. Sankur, and J. Darbon. Shape-based hand recognition. *IEEE Transactions on Image Processing*, 15(7):1803–1815, 2006.

[29] R. L. Zunkel. Hand geometry based verification. *Biometrics*, pages 87–101, 1999.